

# Glioma Detection and Segmentation Using Deep Learning Architectures

M. Gomathi<sup>a\*</sup>, D. Dhanasekaran<sup>b</sup>

<sup>a</sup> Department of Electronics and Communication Engineering, Kings Engineering College, Chennai, India

E-mail: gomathi.nithiarasu@gmail.com

<sup>b</sup> Saveetha School of Engineering, Saveetha Institute of Medical and Technical Sciences, Chennai, India

E-mail: nddsekar@gmail.com

## Article Info

**Page Number:** 452-461

**Publication Issue:**

**Vol. 71 No. 4 (2022)**

## Article History

**Article Received:** 25 March 2022

**Revised:** 30 April 2022

**Accepted:** 15 June 2022

**Publication:** 19 August 2022

## Abstract

Glioma is the primary type of brain tumors which occurred in both human brain regions and spinal cord. It can be cured if it is detected on time by the current scanning methodologies. In this paper, effective Computer Assisted Artificial Methods (CAAM) using deep learning architectures are proposed to differentiate the pixels belonging to Glioma tumors and the pixels belong to non-Glioma tumors. The LeNET and AlexNET deep learning structures along with morphological segmentation procedures are applied on the brain images to detect and locate the tumor pixels in Glioma images. The experimental results are carried out on BRTAS 2019 and BRATS 2020 dataset brain Magnetic Resonance Imaging (MRI). The experimental results of this work are extensively analyzed and compared with similar existing studies.

**Keywords:** Glioma, tumors, CAAM, deep learning, CNN, morphological;

## 1. Introductions

Glioma is the severe type of the brain tumor which is formed over the region of the nervous system of the brain in the human body. This type of tumor can be occurred in either spinal cord or stem of the brain tissues in the brain. There may be different kind of Glioma found from the last two decades. These types of Glioma tumors can be differentiated by the systematic study of symptoms over the long period of tumor detection interval rate. Among the series of systematic symptoms, headache and seizures are the common symptoms in all types of Glioma types [1-3]. The Glioma tumors can be treated by lot of different methods in medical field. Among them, radiation therapy and chemotherapy are very important for treating the tumor pixels in brain. Though these methods are effective in nature for treating the Glioma tumors, the severity levels of the side effects due to these Glioma tumor treating methods are high due to the level of radiation used in these methods. Hence, alternate methods are required to overcome the radiation effect on the brain regions [4-5]. These alternate methods include surgery and molecular therapy. The surgery is the process of removing the tissues belonging to the Glioma tumors in the brain and other regions such as spinal cord also. This surgery method requires accurate Glioma tumor tissues identification. The manual identification of tissues

belonging to Glioma type of tumor is quite complex due to its extreme tissue intensity and illumination levels. Therefore, an effective Computer Assisted Artificial Methods (CAAM) is required to differentiate the pixels belonging to Glioma tumors and the pixels belonging to non-Glioma tumors. The various types of CAAM is illustrated in Fig.1.

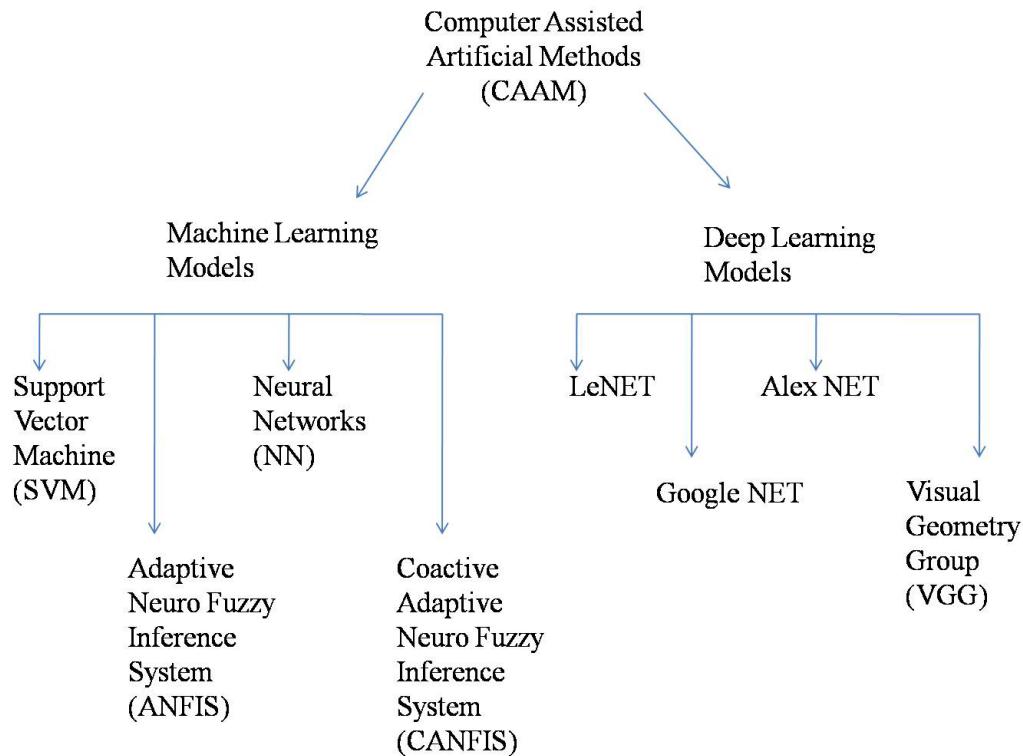


**Figure 1 CAMM types**

This paper applies various CNN architectures for the detection process of Glioma brain tumors. This work divides the entire paper into five sections. The introduction of the Glioma tumors are given in section 1, the existing methods are discussed in section 2, section 3 proposes Glioma brain tumor detection system using various CNN architectures, section 4 is the simulation of the proposed work with respect to various CNN architectures and the final conclusion with future works are stated in section 5.

## 2. Literature Survey

Sahar Gull et al. (2021) developed the customizable CNN architecture for the process of detecting the tumor set of pixels in brain images. This developed method used global threshold technique to locate the non tumor related pixels from the pixels being related with tumor. Then, Google Net CNN architecture was established for training the threshold pixels in the brain images. The authors tested the developed brain tumor pixel segmentation method with the help of the brain images in BRATS 2018, 2019 and 2020 dataset. This method achieved 96% of accuracy rate for BRATS 2018 dataset images and 97% of accuracy rate for BRATS 2019 dataset images and 98% of accuracy rate for BRATS 2020 dataset images respectively. The results were compared with respect to gold standard brain images which were acquired through the radiologist from the recognized health care centers. Methil et al. (2021) provided a solution

for the brain images having illumination problems. The illumination issues in the brain images reduced the detection accuracy of the tumor pixels in the brain images. In order to solve this illumination issues in the brain images, this paper used histogram equalization algorithm for improving the illumination level of each pixel in the brain images. The highly illuminated pixels in the brain images now fed into the classifier which trained and classified the system of brain tumor detection network. The work was regulated by varying the set of illumination static points in the source brain images. Sharif et al. (2020) learned and trained the non-linear pixel pair in source brain image to train the extreme machine learning algorithm. The static pixel features were derived from the trained labels and the mapping between the constructed labels were optimized through this EML algorithm. The developed training approach of the brain tumor detection system was analyzed through the series of testing and validation process to verify the level of accuracy and based on the validation behavior of this system.

Özyurt et al. (2020) detected the cluster pixels in source brain images by clustering the image into various set of non-overlapping regions. The detected cluster pixels in each clustered regions in the brain images were trained by the CNN system for the identification of pixels belonging to abnormal pattern in brain images. This method was tested with only high contrast brain images as the drawback of this developed brain tumor detection system. The authors obtained 96.1% of Tumor Detection Rate (TDR) for the high contrast brain MRI images. Swati et al. (2019) devised transfer learning method for the prediction and level synthesis of various pixel coordinates. The initial training rate of the transfer learning function was found through the threshold function and then the value of the obtained training rate of the transfer function was varied based on the population estimation index rate in this work. The parameters obtained through the transfer learning process were regulated by the fine tuning function. This work was evaluated by the standard validation approaches in this tumor pixel detection algorithm.

Based on the existing algorithms for Glioma detection, deep learning methods are preferred in this paper to identify the Glioma images, as illustrated in Fig.2.

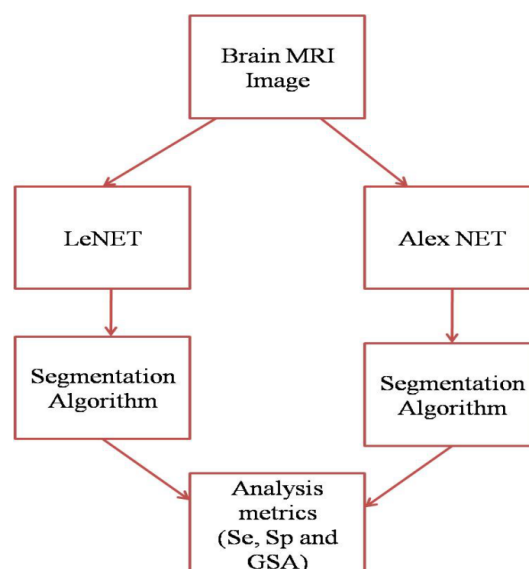


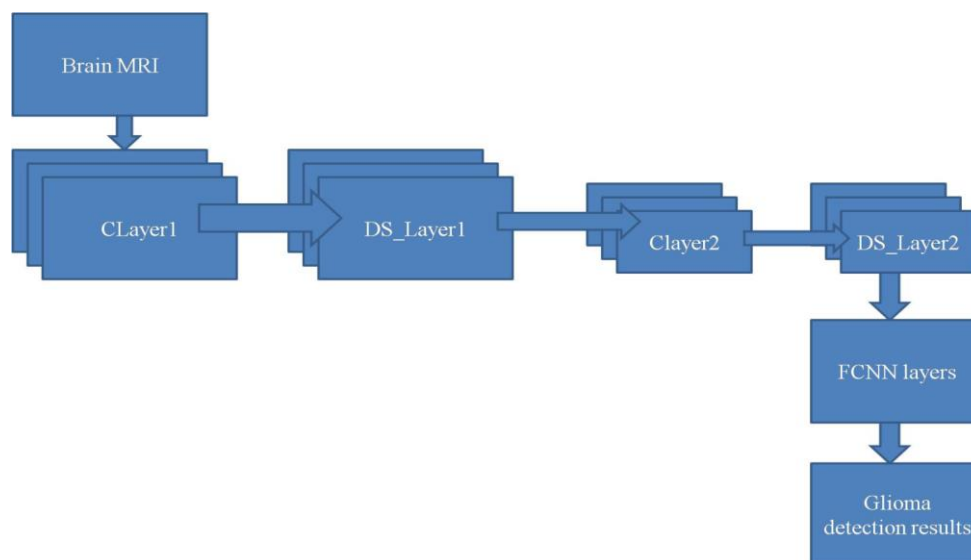
**Figure 2 Methodologies for Glioma detection**

### 3. Proposed Methods

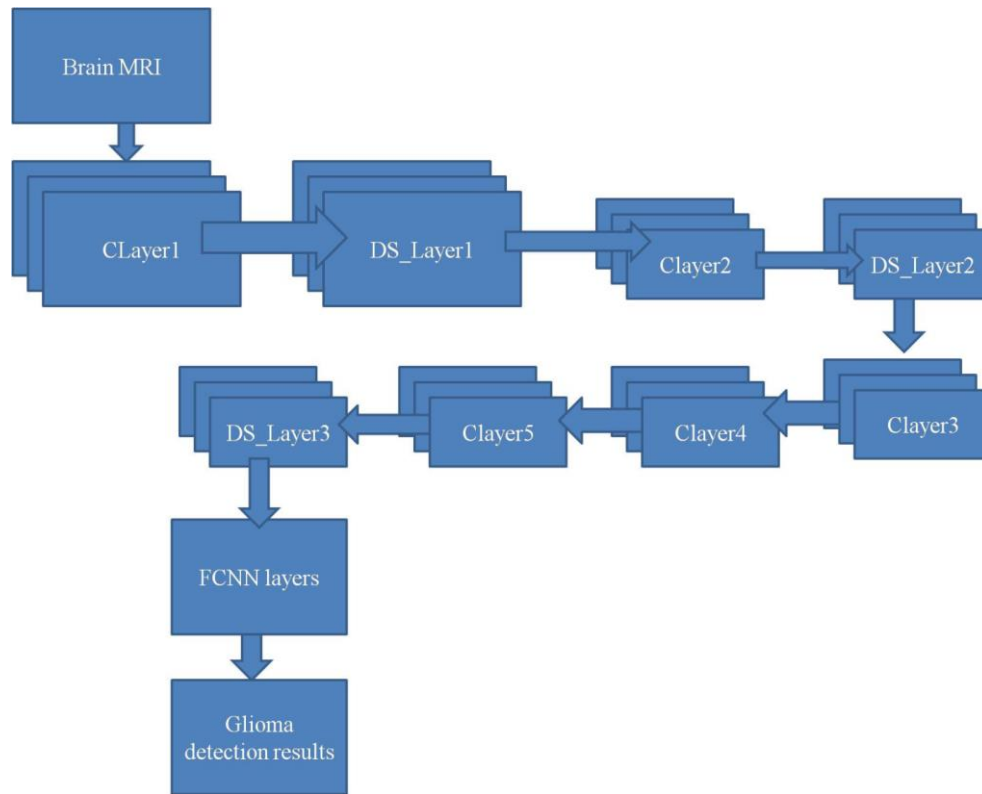
In this paper, deep learning structures LeNET and AlexNET methods (Kestriilia et al. 2019) are applied on the source brain images to detect the Glioma brain image category. The LeNET structure is depicted in Fig. 3(a) and AlexNET structure is depicted in Fig. 3(b) respectively. The deep learning architecture in general methodology consists of Convolutional Layer (C\_Layer) and Down Sampling Layer (DS\_Layer) and Fully Connected Neural Networks (FCNN) with different set of internal neurons in each layers. The LeNET structure used in this design consist of C\_Layer1 and C\_Layer2 with DS\_Layer1 and DS\_Layer2 and three FCNN layers as FCNN1, FCNN2 and FCNN3 respectively (as illustrated in Fig. 3a). The C\_Layer1 consists of 32 filters with  $5 \times 5$  kernel and C\_Layer2 consists of 64 filters with  $5 \times 5$  kernel. The size of convolution response from C\_Layer1 is high and hence DS\_Layer is placed between two C\_Layers in this design. In this paper, Max DS\_Layer is preferred than the Average DS\_Layer due to its minimization of internal losses during the size reduction process. The internally assigned neuron counts for each FCNN layer is depicted in Table 1.

The Alex NET structure used in this design consist of five numbers of C\_Layers (C\_Layer1, C\_Layer2, C\_Layer3, C\_Layer4, C\_Layer5) with three numbers of DS\_Layers (DS\_Layer1, DS\_Layer2 and DS\_Layer3) and three FCNN layers as FCNN1, FCNN2 and FCNN3 respectively (as illustrated in Fig. 3b). The C\_Layer1 consists of 96 filters with  $11 \times 11$  kernel and C\_Layer2 consists of 256 filters with  $5 \times 5$  kernel . C\_Layer3 and C\_Layer4 consist of 384 filters with  $3 \times 3$  kernel respectively and C\_Layer5 consists of 256 filters with  $3 \times 3$  kernel.

The size of convolution response from C\_Layer1 is high and hence DS\_Layer is placed between two C\_Layers in this design. The responses from C\_Layer5 are reduced by DS\_Layer3 and the internal assigned neuron counts for each FCNN layer is depicted in Table 1. The neurons assigned in FCNN3 layer is two which corresponds to Glioma and Healthy brain images.



(a)



(b)

Figure 3 Deep learning CNN structures (a) LeNET (b) Alex NET

Table 1 Specifications of Deep learning CNN structures

| Internal layers | Specifications           |                            |
|-----------------|--------------------------|----------------------------|
|                 | LeNET                    | Alex NET                   |
| C_Layer1        | 32 filters, 5 × 5 kernel | 96 filters, 11 × 11 kernel |
| DS_Layer1       | 2 × 2 Max pooling        | 2 × 2 Max pooling          |
| C_Layer2        | 64 filters, 5 × 5 kernel | 256 filters, 5 × 5 kernel  |
| DS_Layer2       | 2 × 2 Max pooling        | 2 × 2 Max pooling          |
| C_Layer3        | -                        | 384 filters, 3 × 3 kernel  |
| C_Layer4        | -                        | 384 filters, 3 × 3 kernel  |
| C_Layer5        | -                        | 256 filters, 3 × 3 kernel  |
| DS_Layer3       | -                        | 2 × 2 Max pooling          |
| FCNN1           | 120                      | 4096                       |
| FCNN2           | 84                       | 4096                       |
| FCNN3           | 2                        | 2                          |

The Glioma images after classification process through the deep learning structures, morphological open and the morphological close using ‘diameter’ property laid on the Glioma images individually, which produces  $Morp_{open_{image}}$  and  $Morp_{close_{image}}$  respectively. The ‘diameter’ size in open and close function determines the accuracy level of tumor pixel segmentation. After number of iterations, the ‘diameter’ size is fixed in this paper for the

segregation of the abnormal tissues in Glioma images more accurately. The tumor pixels ( $I_{tumor\ pixels}$ ) are segmented using the following Equation.

$$I_{tumor\ pixels} = I(Morp_{open_{image}}) - I(Morp_{close_{image}}) \tag{1}$$

Fig. 4 (a) is the Glioma image and Fig.4 (b) is the tumor pixels located Glioma image.

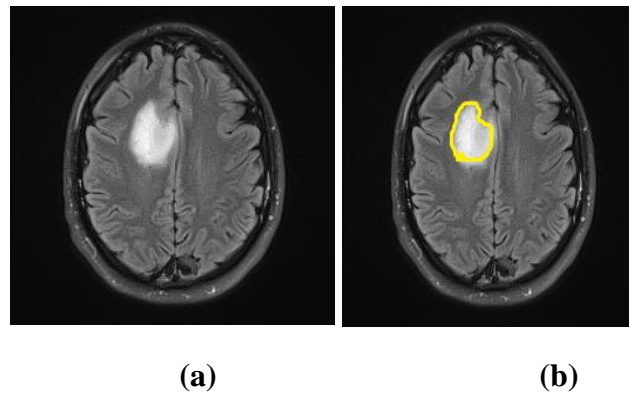


**Figure 4 (a) Glioma image (b) Tumor pixels located Glioma image**

#### 4. Results and Discussions

In this paper, 200 Glioma image samples and 176 Healthy brain images are acquired from BRAT 2019 dataset [12]. Also, 125 Glioma image samples and 189 Healthy brain images are acquired from BRAT 2020 dataset [13]. The proposed Glioma detection method using LeNET and AlexNET are individually applied and tested on both BRATS 2019 and BRATS 2020 dataset to estimate the performance metrics as stated in the Equations (2-4).

$$Sensitivity (Se) = \frac{TRP}{TRP+FAN} \tag{2}$$

$$Specificity (Sp) = \frac{TRN}{TRN+FAP} \tag{3}$$

$$Glioma\ Segmentation\ Accuracy\ (GSA) = \frac{TRP+TRN}{TRP+TRN+FAP+FAN} \tag{4}$$

Whereas, TRP and TRN are the detected pixels belonging to tumor and healthy category correctly, FAP and FAN are the detected pixels belonging to tumor and healthy category incorrectly.

Table 2 is the Glioma detection analysis on BRATS 2019 dataset. The Glioma detection method using LeNET in this paper obtained 95.63% of Se, 94.56% of Sp and 94.4% of GSA. The Glioma detection method using Alex NET in this paper obtained 95.23% of Se, 95.19% of Sp and 96.1% of GSA.

**Table 2 Glioma detection analysis on BRATS 2019 dataset**

| Glioma sequences | LeNET  |        |         | Alex NET |        |         |
|------------------|--------|--------|---------|----------|--------|---------|
|                  | Se (%) | Sp (%) | GSA (%) | Se (%)   | Sp (%) | GSA (%) |
|                  |        |        |         |          |        |         |

|                |              |              |             |              |              |             |
|----------------|--------------|--------------|-------------|--------------|--------------|-------------|
| G19_1          | 97.3         | 94.1         | 94.2        | 94.8         | 95.2         | 94.9        |
| G19_2          | 96.1         | 92.9         | 96.1        | 92.9         | 94.9         | 95.2        |
| G19_3          | 96.3         | 93.1         | 94.2        | 94.9         | 96.2         | 98.4        |
| G19_4          | 95.9         | 94.2         | 94.5        | 95.1         | 94.8         | 93.8        |
| G19_5          | 95.6         | 96.2         | 92.9        | 94.8         | 93.9         | 94.9        |
| G19_6          | 95.2         | 91.2         | 94.1        | 93.9         | 95.8         | 97.2        |
| G19_7          | 94.9         | 95.3         | 93.9        | 96.2         | 93.9         | 94.9        |
| G19_8          | 96.1         | 98.2         | 96.1        | 96.4         | 95.8         | 96.4        |
| G19_9          | 94.2         | 94.3         | 94.2        | 98.2         | 92.9         | 98.2        |
| G19_10         | 94.7         | 96.1         | 93.8        | 95.1         | 98.5         | 97.1        |
| <b>Average</b> | <b>95.63</b> | <b>94.56</b> | <b>94.4</b> | <b>95.23</b> | <b>95.19</b> | <b>96.1</b> |

Table 3 is the Glioma detection analysis on BRATS 2020 dataset. The Glioma detection method using LeNET in this paper obtained 94.56% of Se, 95.32% of Sp and 96.53% of GSA. The Glioma detection method using Alex NET in this paper obtained 94.53% of Se, 95.32% of Sp and 97.88% of GSA.

**Table 3 Glioma detection analysis on BRATS 2020 dataset**

| Glioma sequences | LeNET        |              |              | Alex NET     |              |              |
|------------------|--------------|--------------|--------------|--------------|--------------|--------------|
|                  | Se (%)       | Sp (%)       | GSA (%)      | Se (%)       | Sp (%)       | GSA (%)      |
| G20_1            | 93.8         | 94.9         | 95.8         | 94.2         | 95.3         | 96.1         |
| G20_2            | 94.2         | 92.1         | 96.7         | 94.9         | 95.2         | 97.9         |
| G20_3            | 94.9         | 94.8         | 96.3         | 94.1         | 97.1         | 98.4         |
| G20_4            | 94.8         | 98.2         | 97.1         | 94.3         | 94.3         | 98.8         |
| G20_5            | 93.9         | 96.4         | 95.9         | 95.1         | 95.2         | 98.2         |
| G20_6            | 94.1         | 95.8         | 97.1         | 94.2         | 94.3         | 97.9         |
| G20_7            | 94.9         | 94.7         | 96.8         | 94.9         | 94.9         | 98.3         |
| G20_8            | 92.9         | 96.3         | 96.3         | 94.2         | 95.9         | 97.8         |
| G20_9            | 94.2         | 94.2         | 97.2         | 94.3         | 96.1         | 97.3         |
| G20_10           | 97.9         | 95.8         | 96.1         | 95.1         | 94.9         | 98.1         |
| <b>Average</b>   | <b>94.56</b> | <b>95.32</b> | <b>96.53</b> | <b>94.53</b> | <b>95.32</b> | <b>97.88</b> |

Table 4 is the analysis of Glioma detection methods on BRATS 2019 and BRATS 2020 datasets in terms of metrics using ground truth samples.

**Table 4 Analysis of Glioma detection methods on BRATS 2019 and BRATS 2020 datasets**

| Metrics | BRATS 2019 dataset |          | BRATS 2020 dataset |          |
|---------|--------------------|----------|--------------------|----------|
|         | LeNET              | Alex NET | LeNET              | Alex NET |
| Se (%)  | 95.63              | 95.23    | 94.56              | 94.53    |

|                |       |       |       |       |
|----------------|-------|-------|-------|-------|
|                |       |       |       |       |
| <b>Sp (%)</b>  | 94.56 | 95.19 | 95.32 | 95.32 |
| <b>GSA (%)</b> | 94.4  | 96.1  | 96.53 | 97.88 |

Table 5 and Table 6 are the comparative study of Glioma detection methods on BRATS 2019 and BRATS 2020 dataset images with other similar studies. In this work, the methodologies used in Sahar Gull et al. (2021), Sharif et al. (2020) and Swati et al. (2019) are evaluated on the same number of Glioma image samples which are used in this paper and the results are compared.

**Table 5 Comparative study of Glioma detection methods on BRATS 2019**

| <b>Methods</b>           | <b>Se (%)</b> | <b>Sp (%)</b> | <b>GSA (%)</b> | <b>Methods</b>           | <b>Se (%)</b> | <b>Sp (%)</b> | <b>GSA (%)</b> |
|--------------------------|---------------|---------------|----------------|--------------------------|---------------|---------------|----------------|
| <b>LeNET</b>             | 95.63         | 94.56         | 94.4           | <b>Alex NET</b>          | 95.23         | 95.19         | 96.1           |
| Sahar Gull et al. (2021) | 92.9          | 92.8          | 93.1           | Sahar Gull et al. (2021) | 92.9          | 92.8          | 92.9           |
| Sharif et al. (2020)     | 91.7          | 92.1          | 92.9           | Sharif et al. (2020)     | 93.1          | 91.7          | 92.1           |
| Swati et al. (2019)      | 91.8          | 90.7          | 91.8           | Swati et al. (2019)      | 92.8          | 93.2          | 90.9           |

**Table 6 Comparative study of Glioma detection methods on BRATS 2020**

| <b>Methods</b>           | <b>Se (%)</b> | <b>Sp (%)</b> | <b>GSA (%)</b> | <b>Methods</b>           | <b>Se (%)</b> | <b>Sp (%)</b> | <b>GSA (%)</b> |
|--------------------------|---------------|---------------|----------------|--------------------------|---------------|---------------|----------------|
| <b>LeNET</b>             | 94.56         | 95.32         | 96.53          | <b>Alex NET</b>          | 94.53         | 95.32         | 97.88          |
| Sahar Gull et al. (2021) | 93.1          | 92.9          | 92.8           | Sahar Gull et al. (2021) | 92.8          | 92.8          | 94.2           |
| Sharif et al. (2020)     | 92.9          | 91.7          | 91.7           | Sharif et al. (2020)     | 92.7          | 92.1          | 94.1           |
| Swati et al. (2019)      | 92.1          | 90.5          | 90.6           | Swati et al. (2019)      | 90.4          | 90.9          | 93.2           |

## 5. Conclusions

In this work, deep learning structures LeNET and Alex NET are used to detect the Glioma images. The Glioma detection method using LeNET in this paper obtained 95.63% of Se, 94.56% of Sp and 94.4% of GSA for BRATS 2019 dataset images. The Glioma detection

method using Alex NET in this paper obtained 95.23% of Se, 95.19% of Sp and 96.1% of GSA. The Glioma detection method using LeNET in this paper obtained 94.56% of Se, 95.32% of Sp and 96.53% of GSA for BRATS 2020 dataset images. The Glioma detection method using Alex NET in this paper obtained 94.53% of Se, 95.32% of Sp and 97.88% of GSA. The experimental results of both dataset are compared with Sahar Gull et al. (2021), Sharif et al. (2020) and Swati et al. (2019). The present deep learning structure will be customized in future to improve the experimental results for Glioma detection.

## References

1. Kamnitsas, K., Ledig, C., Newcombe, V.F.J., Simpson, J.P., Kane, A.D., Menon, D.K., Rueckert, D., Glocker, B.: Efficient multi-scale 3D CNN with fully connected CRF for accurate brain lesion segmentation. *Med. Image Anal.* 36, 61–78 (2017).
2. Zikic, D., Glocker, B., Konukoglu, E., Criminisi, A., Demiralp, C., Shotton, J., Thomas, O.M., Das, T., Jena, R., Price, S.J.: Decision forests for tissue-specific segmentation of high-grade gliomas in multi-channel MR. In: MICCAI, pp 369–376 (2012).
3. Bauer, S., Wiest, R., Nolte, L., Reyes, M.: A survey of mri-based medical image analysis for brain tumor studies. *Phys. Med. Biol.* 58, 97–129 (2013).
4. Pereira, S., Pinto, A., Alves, V., Silva, CA.: Brain tumor segmentation using convolutional neural networks in MRI images. *IEEE Trans. Med. Imaging* 5, 1240–1251 (2016).
5. M. Toğaçar, B. Ergen, and Z. Cömert, “BrainMRNet: brain tumor detection using magnetic resonance images with a novel convolutional neural network model,” *Medical Hypotheses*, vol. 134, article 109531, 2020.
6. Kestrelia R. Prilianti, Tatas Brotosudarmo, Syaiful Anam, “Performance comparison of the convolutional neural network optimizer for photosynthetic pigments prediction on plant digital image”, *AIP Conference Proceedings*, Vol.2084, no. 1, 2018.
7. Sahar Gull, Shahzad Akbar, Habib Ullah Khan, "Automated Detection of Brain Tumor through Magnetic Resonance Images Using Convolutional Neural Network", *BioMed Research International*, vol. 2021, Article ID 3365043, 14 pages, 2021.
8. M. A. Sharif, J. Amin, M. Raza, M. A. Anjum, H. Afzal, and S. A. Shad, “Brain tumor detection based on extreme learning,” *Neural Computing Applications*, vol. 32, no. 20, pp. 15975–15987, 2020.
9. Meneses-Claudio, B., Nuñez-Tapia, L., Alvarado-Díaz, W.,”Detection of Possible COVID-19 Cases using Thermal Imaging and a DRONE”,
10. (2022) *International Journal of Emerging Technology and Advanced Engineering*, ISSN: 22502459, 12 (1), pp. 129-137.

11. Perez-Siguas, R., Matta-Solis, E., Matta-Solis, H., "Design of a Body Temperature Measurement System applied to Health Center Personnel", (2022) International Journal of Emerging Technology and Advanced Engineering, ISSN: 22502459, 12 (2), pp. 20-28.
12. F. S. Özyurt, E. Sert, and D. Avcı, "An expert system for brain tumor detection: fuzzy C-means with super resolution and convolutional neural network with extreme learning machine," Medical Hypotheses, vol. 134, article 109433, 2020.
13. Z. N. K. Swati, Q. Zhao, M. Kabir et al., "Brain tumor classification for MR images using transfer learning and fine-tuning," Computerized Medical Imaging and Graphics, vol. 75, pp. 34–46, 2019.
14. S. Methil, "Brain Tumor Detection using Deep Learning and Image Processing," 2021 International Conference on Artificial Intelligence and Smart Systems (ICAIS), 2021, pp. 100-108.
15. BRATS 2019 dataset: <https://www.kaggle.com/general/40301>
16. BRATS 2020 dataset: <https://github.com/akhanss/BraTS-2020>